

## Integrated Simulations for Imploded Core Heating in Fast Ignition

T. Johzaki<sup>1</sup>, H. Nagatomo<sup>1</sup>, H. Sakagami<sup>2</sup>, T. Nakamura<sup>1</sup>, K. Mima<sup>1</sup>, Y. Nakao<sup>3</sup>

<sup>1</sup> *Institute of Laser Engineering, Osaka University, Osaka 565-0871, Japan*

<sup>2</sup> *Theory and Computer Simulation Center, National Institute for Fusion Science, Toki  
509-5292, Japan*

<sup>3</sup> *Department of Applied Quantum Physics and Nuclear Engineering, Kyushu University,  
Fukuoka 812-8581, Japan*

### 1. INTRODUCTION

In fast ignition scheme, the clarification of core heating mechanism is one of the most important issues. To simulate the overall physics and identify the crucial physics in the core heating, we developed an integrated code system “Fast Ignition Integrated Interconnecting code” (FI<sup>3</sup> code) [1], which includes all-important physics from the implosion to the core heating. The overall implosion dynamics is simulated by an ALE-CIP radiation-hydro code “PINOCO” [2]. A collective PIC code “FISCOF” [3] simulates the relativistic laser-plasma interactions (LPI) to evaluate the time-dependent energy distribution of relativistic electron beam. The core heating is simulated with a relativistic Fokker-Planck (FP) code coupled with hydro-based burn simulation code “FIBMET” [4].

In the previous work [5], on the basis of integrated simulations with FI<sup>3</sup> code for fast heating experiments with cone-guided CD shell targets [6], we found the density gap effects on fast electron transport. If the plasma density between cone tip and dense core is low such as  $10n_c$  ( $n_c$  is laser critical density), the strong two stream instability is induced there due to fast electron flow, which generates the strong static field. Due to this field, some of fast electrons having relatively low energy are trapped inside the cone tip and bulk electrons are accelerated toward the cone tip. These confined moderate-energy fast electrons are gradually released from the cone tip with intensity of  $\sim 10^{18}\text{W/cm}^2$  even after laser irradiation and contribute to the core heating. Thus, if such low dense plasma exists between cone tip and core plasma, the profiles of fast electrons generated by ultra-intense laser irradiation change during propagation into the core, *i.e.* the energy spectrum is moderated and the electron beam duration becomes longer. As the results, core heating efficiency becomes high compared with the no density gap case. Even if including the density gap effect, however, the resultant ion temperature reaches only 0.45keV, which is still lower than the value obtained in the experiments (0.8keV) [5].

In the heating phase of fast ignition, before main pulse irradiation, low density plasma is formed on the cone inner surface due to the pre-pulse, of which scale length may affect fast electron spectrum. In the previous simulations, we fixed pre-plasma scale length as  $L_f = 5\mu\text{m}$  for the cone tip surface. In the present paper, we evaluate the pre-plasma scale length dependence of core heating efficiency.

## 2. SIMULATION CONDITION

First, we carried out implosion simulations for an Au cone attached CH shell target to obtain the compressed core profile. For heating phase, time-dependent profile of fast electron injected into dense core is evaluated with PIC simulations and the following energy transport in the dense core is simulated by the FP code. In the core heating, the multi-dimensional natures, *e.g.* geometrical effects of laser-cone interactions, magnetic field effects, spatial beam divergence, are off cause important. However, full scale (time and space) multi-dimensional simulation is very expensive. Thus, for the present parameter study on scale length dependence, we used 1-dimensional (1D) PIC and FP codes.

## 3. PRE-PLASMA SCALE LENGTH DEPENDENT

### 3.1 Fast Electron Profiles

For evaluation of fast electron profiles, we carried out 1D PIC simulations where electrons and ions (Au,  $Z=50$ ) are mobile and the collision process is not included. The cone tip is modelled by  $100n_c$  and  $10\mu\text{m}$  thickness plasma. The pre-plasma having exponential density profile ( $n_e \propto \exp(x/L_f)$ ,  $L_f$  is scale length) is attached to the front surface. On the rear surface of the cone tip, we located  $24\mu\text{m}$  thickness imploded plasma with exponential profile of scale length  $L_r = 10\mu\text{m}$ . The density is varied from  $n_e = 10n_c$  at the contact surface to  $100n_c$  at  $24\mu\text{m}$  behind the rear surface. Following the imploded plasma, a  $100n_c$ ,  $26\mu\text{m}$  plasma is located as the dense core. The heating laser is the Gaussian pulse with  $\lambda_L = 1.06\mu\text{m}$ ,  $\tau_{\text{FWHM}} = 750\text{fs}$  and  $I_L = 10^{20}\text{W/cm}^2$ . The irradiated laser energy is  $0.79\text{J}/\mu\text{m}^2$ , which corresponds to  $560\text{J}$  when the laser spot size is  $15\mu\text{m}$ . The simulation time is  $6\text{ps}$ .

In Fig.1, we show the fast electrons profiles, (a) time-integrated energy spectra and (b) temporal profile of beam intensity, observed at  $20n_c$  point of the rear plasma are plotted for  $L_f = 0\mu\text{m}$ ,  $0.25\mu\text{m}$ ,  $1\mu\text{m}$  and  $5\mu\text{m}$  cases. With increasing  $L_f$ , the pre-plasma has longer underdense region, which means the laser-plasma interaction region becomes long. Thus, the generated fast electron energy becomes high (Fig.1(a)). As is found in Fig.1 (b), the temporal profiles of electron beam intensity during laser irradiation ( $t = 0 \sim 2.5\text{ps}$ ) are similar to that of laser pulse. During this phase, relatively high-energy fast electrons flow toward the core. Due to the fast electron current, the static field is built up at the cone tip - plasma interface, and the

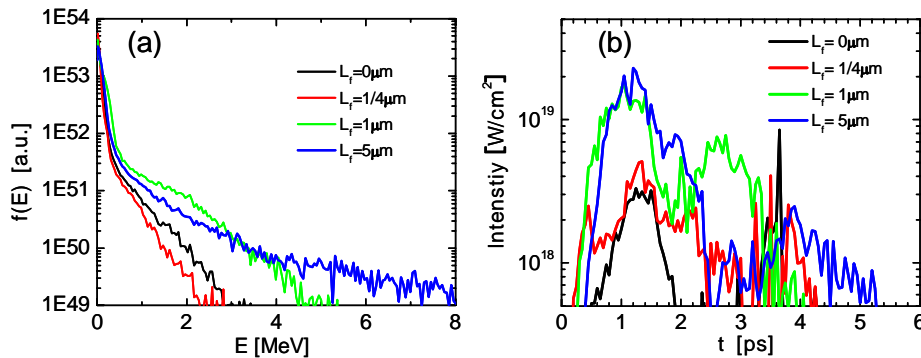


Fig.1 Fast electron profiles obtained by 1D PIC simulations for  $L_f = 0, 0.25, 1, 5\mu\text{m}$  cases. (a) time-integrated energy spectra, (b) temporal profiles of electron beam intensity.

relatively low-energy fast electrons are trapped in the cone tip and the bulk electrons are accelerated into the cone tip. These trapped electrons are scattered at the laser-plasma interaction region and accelerated toward the core. Thus some of fast electrons are confined inside the cone tip and they are gradually released even after laser irradiation with beam intensity of  $10^{18}\text{W}/\text{cm}^2$  level.

### 3.2 Core heating

Using the time-dependent profiles of fast electron after passing through the low-density gap region, we carried out the core heating simulations using the 1D FP code. As for the bulk plasma profile, we use the imploded core profiles at the central axis ( $r = 0$ ) obtained by r-z cylindrical 2D implosion simulation with PINOCO. The fast electrons are injected behind the cone tip (between the cone tip and the dense core).

In Fig.2, spatial profiles of fast electron energy deposition at  $t = 2.5\text{ps}$  are plotted for the  $L_f = 1.0\mu\text{m}$  case. In the low-density region around the fast electron injection point, the Joule heating is comparable to the collisional heating due to the Coulomb interactions with bulk electrons. In the dense core region, the fast electron current can be easily cancelled by bulk electron flow with small drift velocity ( $v_d \ll c$ ) because of much larger density of bulk electron than that of fast electron, so that the field effect is negligible and the collisional heating is dominant. The temporal evolution of ion and electron temperatures averaged over  $\rho > 10\text{g}/\text{cm}^3$  region,  $\langle T_k \rangle = \int_{\rho > 10\text{g}/\text{cm}^3} T_k(x) R_{DT}(x) dx / \int_{\rho > 10\text{g}/\text{cm}^3} R_{DT}(x) dx$  where  $k$  denotes ion or electrons and  $R_{DT}(x)$  is DT reaction rate at position  $x$ , are shown in Fig.3 for the case of  $L_f = 1\mu\text{m}$ . Due to the collisional heating, the bulk electron is heated first, and then the bulk ion is heated via the temperature relaxation. Thus, the electron temperature reaches maximum ( $\langle T_e \rangle_{\text{max}} = 0.84\text{keV}$ ) at  $t = 3.6\text{ps}$ , and then  $\langle T_i \rangle_{\text{max}} = 0.72\text{keV}$  is obtained by 3ps delay.

The results of core heating simulations by varying  $L_f$  are summarized in Fig.4. Fig.4 (a) shows the scale length dependence of time-integrated energy of the fast electron beam (total and  $E < 2\text{MeV}$  component) and the energy deposited by fast electron inside the fuel plasma. The right axis indicates the energy coupling from laser to each value. In Fig.4(b), the maximum value of  $\langle T_i \rangle$  is plotted as a function of  $L_f$ . With increasing  $L_f$  up to  $1.5\mu\text{m}$ , the energy coupling from heating laser to fast electron becomes larger, so that the deposited

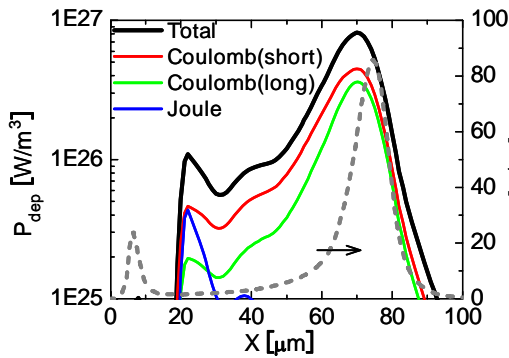


Fig.2 Energy deposition profile of fast electron at  $t = 2.5\text{ps}$  for the case of  $L_f = 1\mu\text{m}$ .

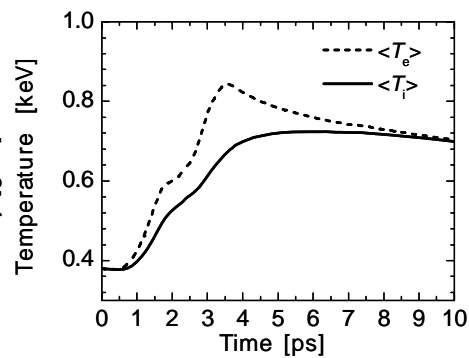


Fig.3 Temporal evolution of ion and electron temperature averaged over dense core region ( $\rho > 10\text{g}/\text{cm}^3$ ) in the case of  $L_f = 1\mu\text{m}$ .

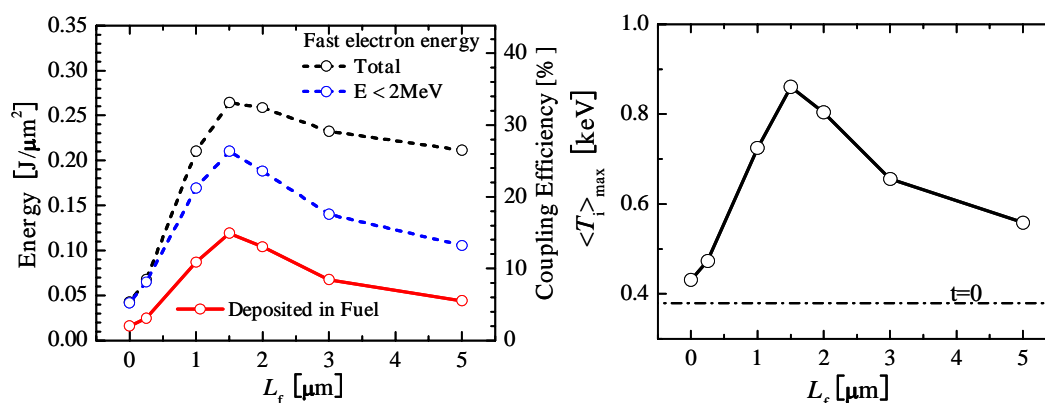


Fig.4 Pre-plasma scale dependence of (a) total fast electron energy (black) and its  $E < 2\text{MeV}$  component (blue) and deposited energy of fast electron inside the fuel, and (b) maximum value of core ion temperature  $\langle T_i \rangle_{\text{max}}$ .

energy and the resultant core temperature increase. The scale length becomes long furthermore, the total beam energy gradually decreases. However, the higher energy component ( $E > 2\text{MeV}$ ) increases, so that the low energy component ( $E < 2\text{MeV}$ ), which is effective in core heating, decreases faster than the total beam energy. As the result, the deposited energy in the fuel plasma and the resultant core temperature also decrease. These results indicate that the core heating efficiency depends not on the total beam energy but on the beam energy of low energy component ( $E < 2\text{MeV}$ ), *e.g.* in the case of  $L_f = 1\mu\text{m}$ , though the total beam energy is comparable to the case of  $L_f = 5\mu\text{m}$ , the beam energy of  $E < 2\text{MeV}$  component is 1.5 times as large, and then  $\langle T_i \rangle_{\text{max}}$  is higher by 0.17keV. In the present simulations, the optimum scale length for core heating is  $L_f = 1.5\mu\text{m}$ . In this case, the energy coupling from the heating laser to the core is 14.9% and ion in the core is heated up to 0.86keV (0.48keV rising). In the region of  $1\mu\text{m} \leq L_f \leq 2\mu\text{m}$ , the heated core temperature is comparable to the value obtained at the experiments.

#### 4. CONCLUDING REMARKS

On the basis of 1D integrated simulations, we found that the pre-plasma scale length strongly affects the fast electron generation and then the core heating efficiency. In the present study, the optimum scale length is  $L_f = 1.5\mu\text{m}$ , and the energy coupling from heating laser to core of 14.9% and heated core temperature of 0.86keV are achieved. For further study, experimental measurement or simulation prediction is required for pre-plasma profile.

#### 5. REFERENCES

- [1] H. Sakagami and K. Mima, *Laser Part. Beams*, 22 (2004) 41.
- [2] H. Nagatomo et al., *Proc. of 2nd IFSA (Kyoto, 2001)*, Elsevier, 140 (2001).
- [3] H. Sakagami et al., *Proc. of 3rd IFSA (Monterey, 2003)*, ANS, 434 (2004).
- [4] T. Johzaki et al., *J. Plasma Fusion Res. SERIES*, 6 (2004) 341; T. Yokota, et al., *Phys. Plasmas* 13, (2006) 022702.
- [5] T. Johzaki et al., "Core Heating Analysis of Fast Ignition Targets by Integrated Simulations" to be published in *J. Phys. Conference Series (Proc. IFSA2005)*.
- [6] R. Kodama et al., *Nature*, 412, 798 (2001); *ibid.*, 418, 933 (2002).